Hindawi
Journal of Spectroscopy
Volume 2020, Article ID 1402965, 7 pages
https://doi.org/10.1155/2020/1402965

Research Article

The Kinetic Model of the Peel Brittleness of Stored Cucumis Melons Based on Visible/Near-Infrared Spectroscopy

Defang Xu,[1] Huamin Zhao,[1] Shujuan Zhang,[1] Chengji Li,[1] and Fei Zhao[2]

[1]*College of Engineering, Shanxi Agricultural University, Taigu County, Jinzhong 030801, Shanxi, China*
[2]*Shanxi Agricultural Machinery Development Center, Shanxi, Taiyuan 030002, China*

Correspondence should be addressed to Huamin Zhao; zhaohuamin909@163.com and Shujuan Zhang; zsujuan1@163.com

Received 5 October 2019; Accepted 3 January 2020; Published 28 January 2020

Academic Editor: Wee Chew

A kinetic model based on visible/near-infrared spectroscopy of the peel brittleness of "Xintian-125" Cucumis melons, the research object, stored under room temperature, was established in order to realize real-time monitoring of the peel brittleness of Cucumis melons and for prediction of storage time. The NIR and peel brittleness of melons stored for 1, 4, and 7 days were collected and measured. SG was confirmed to be the best pretreatment by comparing the PLS models established with 4 pretreatment methods, and the differences of the prediction set determination coefficient and root-mean-square were 0.818 and 23.755, respectively. CARS and SPA were adopted to extract the feature wavelengths and establish the peel brittleness of PLS prediction model. The model's prediction accuracy was 0.919, and the prediction root-mean-square was 25.413, indicating that NIR is able to realize the prediction of the peel brittleness of Cucumis melons. As a result, a NIR-based peel brittleness kinetic model was created. The P value of the regression model was less than 0.001, and the model's correlation coefficient was 0.8503, showing that the model is of extreme significance and high precision. The zero-order reaction equation was overfitted according to the variation tendency of the average peel brittleness of stored melons. The model's correlation coefficient was 0.981, the standard error was 4.624, and the linear relation between the stored period and NIR was established based on it. The research proves that the NIR-based technology is able to realize quick and loss-free inspection of melons' peel brittleness and prediction of the stored period.

1. Introduction

Cucumis melon ("Melon"), also known as muskmelon, is an annual vine herb of Cucurbitaceae. It is crunchy, sweet, and juicy as well as rich in nutrition. And it is one of the top ten fruits available in the international market [1]. Different from other fruits, melon is prone to the loss of the best flavor at room temperature after the picking time due to its high water content, high sugar content, strong physiological metabolism, short storage period, and harsh storage conditions [2]. How to ensure that consumers can buy sweet and crisp melon is of great importance. Peel brittleness is an important indicator affecting the flavor and quality of melon. During the storage at room temperature, water gets lost as a result of the respiration and transpiration of melon. Pectin and cellulose are continuously consumed and reduced due to hydrolysis, and fruit constantly softens because of cell dissolution and cell wall metabolism. The changes in these indicators not only determine the fruit peel friability but also affect its absorption peak of the spectrum. On this account, the relationship model between visible/near-infrared spectroscopy (Vis/NIR) and the melon peel crispness during storage is studied here, in an effort to find a method that can quickly and nondestructively determine the storage period of melon with thin peel.

NIR spectroscopy is generated at the time of molecular vibration transition from the ground state to a higher energy level with the help of the vibration nonresonance. This mainly reflects the frequency doubling and combination absorption of the stretching vibration of hydrogen-containing groups [3]. It has received much attention from researchers because of its unique fast, efficient, pollution-free, and nondestructive advantages. Peirs et al. [4] used the Vis/NIR spectroscopy to study apple maturity. The results

showed that, in the prediction model of apple maturity, the R value and the SEP value were 0.90 and 7.4 d, respectively, and a PLS correction model was established. Ignat et al. [5] used the Vis/NIR spectroscopy to detect the internal quality parameters of apples during picking and storage. The results showed that the method could better predict the internal quality changes of apples during storage. Li et al. [6] used Vis/NIR to determine the SSC content of different pear varieties. The results showed that the nonlinear LS-SVM model predicted the SSC content of pears due to the linear PLS model. He et al. [7] used the Vis/NIR hyperspectral imaging to predict the VC content of Lingwu long jujube. The results showed that the PLS model based on CARS had the best effect. Munera et al. [8] used the spectral and spatial information to establish classification models of persimmons with different maturity and astringency levels and predicted the maturity and convergence by multivariate analysis techniques such as linear and quadratic discriminant analysis (LDA and QDA) and support vector machine (SVM), with the correct classification rate of more than 95%. Abdullah M. Alhamdan et al. used Vis/NIR to study the correlation between the five maturity levels of Barhi dates and near-infrared. The study found that the correlation coefficient (R2) between the quality parameter of Barhi dates and TSS (total soluble solid) was 0.97; the correlation coefficient was 0.94; and the correlation coefficient of b^* color was 0.64. In addition, many scholars have studied the methods to detect the classification, quality, and maturity of common fruits such as grapes [9, 10], citrus [11], olive [12], tomato [13], mango [14], and Melon with thick peel [15] by using the NIR spectroscopy in combination with the parameters of soluble solids content or image information of the fruits. However, there are few studies on the detection of NIR shelf life of melon with thin peel. It was found in previous studies that it would be simple and accurate in expression to use the PCA, CARS, and SPA methods to extract characteristic wavelengths and then the PLS method to establish regression models. Therefore, taking melon as the subject, according to the change in the friability of the peel during storage, a kinetic model of melon peel during storage was established in this paper to predict the length of melon storage period so as to provide theoretical support for consumers to quickly and nondestructively determine the freshness of melon.

2. Experimental Materials and Methods

2.1. Experimental Materials. "Xintian-125" melons harvested from the Cucumis melon planation of Taigu County, Shanxi Province, were used as the test object. The preexperiment showed that the ripe samples were harvested and stored under room temperature (20°C), the melons softened the 7th day, and the decrease in peel brittleness was obvious, indicating the loss of their edible quality, so the test storage period was 7 days. The samples were transported to the laboratory after harvest; 255 samples with even textures were selected after two hours of standing, which showed no insect attack, and were numbered and labeled. The samples were divided into 3 groups, and each group contained 85 melons. The spectral information of all samples was collected in the first day, and the peel brittleness of the first group was measured. Then, the spectral information and peel brittleness of the second and third groups were collected and measured in the fourth and seventh days. Kennard-Stone [16–18] was employed to divide the samples into a calibration set and a prediction set according the ratio of 3 : 1, namely, 64 calibration sets and 21 prediction sets in each group.

2.2. Collection of Spectral Data. Field Spec 3 spectrometer (Analytical Spectral Device, USA) was used to collect the visible/near-infrared spectral data of samples. The spectral resolution was 3.5 nm@700 nm and 10 nm@1400 nm and 2100 nm, the spectral band range was 350~2500 nm, and the interval of each wave band data collection was 1 nm. In order to reduce the influence of spectral acquisition location, the maximum transverse diameter of each sample was scanned for 3 times. As shown in Figure 1, points 1, 2, and 3 on the melon are the spectral acquisition locations and View Spec Pro was used to calculate the average spectral values. The experiment collection equipment is shown in Figure 1.

2.3. Measurement of Peel Brittleness. TA-XT-plus Texture Exponent 32 (Stable Micro System, the UK) was used to measure the peel brittleness of samples. A P/2n needle-shaped probe, with the diameter of 2 mm, was used to pierce through the melons, and the puncture point corresponded to the point of spectral data collection. The rate of descent of the probe before the puncture was 3 mm/s, and the puncture rate was 1.5 mm/s. The return rate was 10 mm/s after the puncture was finished, and the puncture distance was 5 mm with a trigger force which was 5 g. The statistics of the peel brittleness of melons stored for different days are shown in Table 1. The table showed an obvious decrease in peel brittleness of the melons during storage.

2.4. Data Processing and Analysis Software. Software including View Spec Pro (Analytical Spectral Device, USA), Matlab R2012a (The MathWorks, Natick, USA), the Unscrambler X10.1 (CAMO ASA, Trondheim, Norway), SAS (SAS INSTITUTE INC, USA), and Origin8.5 (Origin Lab, USA) was used in the research to process and analyze the data.

3. Data Analysis and Model Establishment

3.1. Spectral Analysis of Melons in Different Storage Periods. The spectral data that corresponded to 450~2400 nm were used for analysis since the SNR within 350~450 nm and 2400~2500 nm was low and noise was high among the 350~2500 nm wave band. The average spectral curves of NIR for melons in different storage periods are shown in Figure 2.

Figure 2 shows that the spectral curves of melons in different storage periods all exhibited significant sunken absorption peaks close to 977 nm, 1201 nm, 1479 nm, 1793 nm, and 1933 nm. The research conducted by Polesello

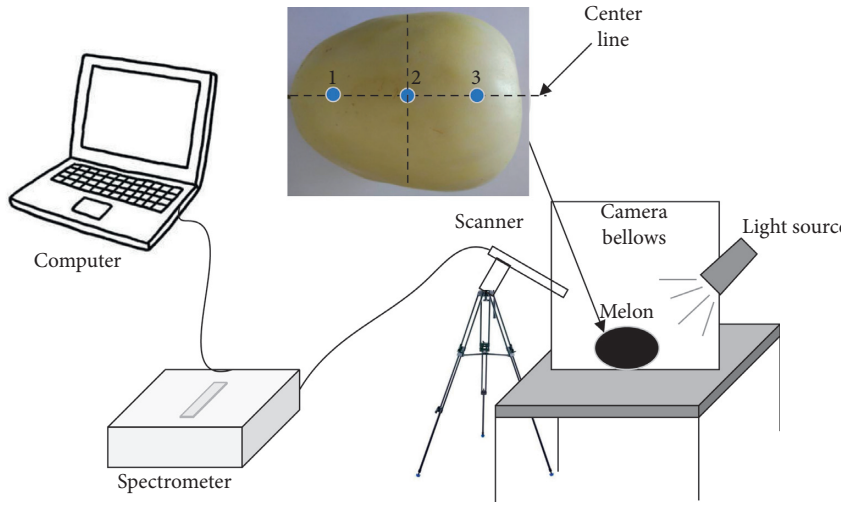

Figure 1: The experiment collection equipment and measuring position of melon.

Table 1: Statistical results of the peel brittleness of Cucumis melons during storage.

Storage period (d)	Max.	Min.	Average	Standard deviation
1	579.35	348.44	460.37	62.53
4	555.90	279.58	391.61	63.71
7	469.25	176.14	313.00	66.73

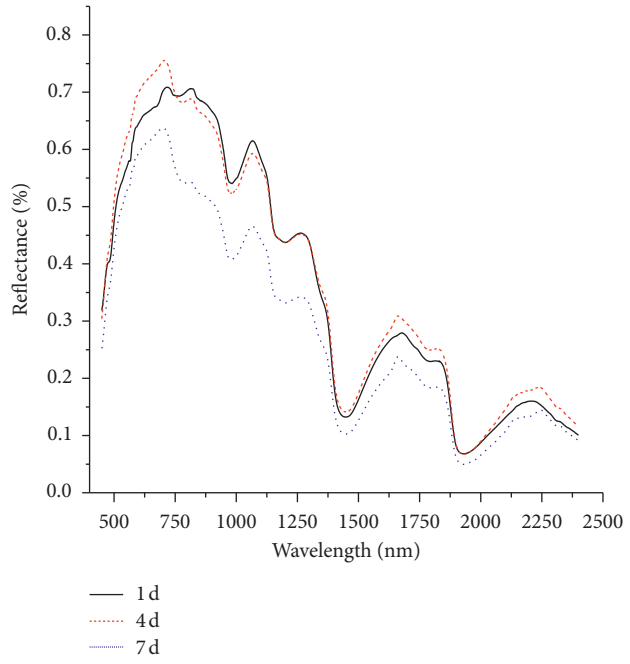

Figure 2: Mean spectrum chart of Cucumis melons in different storage periods.

et al. [19] showed that the absorption peaks of water emerged in positions when the wave bands were 970, 1190, 1450, 1780, and 1940 nm. Among them, the combined O-H absorption peak that appeared when the wave band was 1190 nm and 1450 nm was the level-one doubled frequency of the stretching vibration of O-H, and 1940 nm was the level-two doubled frequency of the stretching vibration of O-H. It could be found from Figure 2 that, on the 7th day, the decrease rate of the reflectance in the main absorption peak area of water was significantly greater than that of the nonaqueous absorption peak area. It could be thus judged that water was greatly lost in melon at 7 days during storage.

3.2. Establishment of NIR Kinetic Model for the Peel Brittleness of Cucumis Melons

3.2.1. Spectral Pretreatment. Lots of irrelevant redundant information exist in the original full spectral wave band, which may affect the accuracy and prediction effect of the established model [20]. Different pretreatment methods lead to different accuracies of the established models. This paper selected the following common and effective preprocessing methods:

(1) *Savitzky–Golay (SG) Smoothing*. The least squares fitting coefficient is used in the digital filtering corresponding function of this method, and it is essentially a weighted average method by eliminating noise with convolution smoothing.

(2) *Baseline Correction*. It is mainly used to eliminate the effect of baseline drift caused by other factors such as sample inhomogeneity and instrument background. The corrected spectrum is obtained by finding the spectral value of the smallest wavelength of each sample and using it as the baseline and then subtracting the baseline value from the spectral values of all wavelengths.

(3) *Standard Normalized Variate (SNV) Algorithm*. It performs standard normalization on the absorbance value at the wavelength of the spectrum to meet the normal distribution and then corrects the spectral data of the experimental samples on this basis.

(4) *Multiplicative Scatter Correction (MSC)*. It is mainly used to eliminate the scattering effect in reflection spectrum and diffusion projection. The spectral

absorption signal related to component content is enhanced. The average spectrum of the correction set is used as an approximately ideal spectrum. The absorbance value at any wavelength point of each sample is approximately linear with the corresponding absorbance of the ideal one. The intercept and slope of the line can be linearly and regressively calculated through the spectrum to correct each spectrum.

PLS model was established via the preprocessed data to compare the model accuracy and select the optimal preprocessing method. Table 2 shows the results of the PLS model established by different preprocessing methods. According to the results in Table 2, the accuracy of the model after SG pretreatment was the best and confirmed as the best pretreatment. The determination coefficients of the model's calibration set and prediction set R_c^2 and R_p^2 were, respectively, 0.884 and 0.818, and the root-mean-square errors RMSEC and RMSEP were, respectively, 22.205 and 23.775.

3.2.2. Extraction of Feature Wavelengths. The algorithm time is not only increased but also the prediction precision of models is weakened since the volume of original spectral data of samples is enormous and large amounts of information unrelated to the measured groups are included in spectral analysis [21]. Therefore, the original spectral data shall be optimized, and effective variables of wavelengths shall be extracted.

CARS [22, 23] employs cross validation (CV) to single out the sublets with the minimum RMSECV values. The frequency of Monte Carlo sampling was set as 50, and the running result is shown in Figure 3. The RMSECV of the model tended to minimize when the sampling frequency was 24, and extracted feature wavelengths at this time were 481, 483, 484, 485, 486, 492, 530, 531, 533, 537, 563, 571, 828, 829, 830, 840, 841, 1089, 1090, 1091, 1092, 1094, 1095, 1096, 1097, 1098, 1103, 1104, 1105, 1106, 1302, 1305, 1307, 1308, 1309, 1310, 1311, 1340, 1341, 1345, 1358, 1360, 1361, 1362, 1363, 1509, 1510, 1910, 1911, 1912, 1913, 1914, 1915, 1916, 1917, 1918, 1919, 1920, 1921, 1926, 1933, 1937, 2126, 2127, 2128, 2131, 2132, 2134, 2135, 2138, 2140, 2155, 2158, 2159, 2160, 2161, and 2168 nm, with a total of 77. Obviously, the quantity of extracted feature wavelengths still remained huge, which did not help to establish the kinetic model of peel brittleness. Hence, feature wavelengths were once again extracted.

Successive projection algorithm (SPA) [24–26] is able to locate the variable group with the lowest limit of redundant data from spectral data, thus minimizing the collinearity among variables. The result is shown in Figure 4. The total quantity of the best characteristic parameters was 9, as confirmed by the internal CV RMS errors of calibration sets, which were 1106, 841, 1340, 1917, 530, 1933, 1302, 2159, and 480 nm, and their importance level descended in this order.

3.2.3. Establishment of the Kinetic Model for Peel Brittleness. 9 feature wavelengths extracted by CARS-SPA were selected to establish the PLS prediction model for the peel brittleness of Cucumis melon, as shown in Figure 5. The prediction accuracy of the model R_p was 0.919, and the prediction RMSEP was 25.413, indicating that NIR-based technology is able to detect the peel brittleness of melons.

Table 2: Prediction results of PLS prediction model about peel brittleness with different pretreatment consequences.

Pretreatment methods	R_c^2	RMSEC	R_p^2	RMSEP
SG	0.884	22.205	0.818	23.775
Baseline	0.846	25.520	0.760	27.577
SNV	0.816	27.897	0.667	31.429
MSC	0.816	27.894	0.668	31.397

9 feature wavelengths above were selected, and the NIR peel brittleness kinetic model of Cucumis melons was established based on multivariate regression analysis in SAS. The model expression was shown as equation (1), while the analysis of variance in regression is shown in Table 3. The P value of the regression model was less than 0.001, and the determination coefficient was 0.8503, which means that the model is of extreme significance and high precision:

$$\begin{aligned} A = &-4318.395X_1 + 4106.842X_2 - 4215.299X_3 \\ &+ 9399.809X_4 - 4438.19X_5 - 6481.062X_6 - 20907X_7 \\ &+ 11692X_8 + 11784X_9 + 527.963, \end{aligned} \tag{1}$$

where A is the peel brittleness value, while $X_1 \sim X_9$ indicate the absorbance levels corresponding to each feature wavelength.

3.3. Establishment of the Kinetic Model for Peel Brittleness of Stored Cucumis Melons. While processing and storing foods, most quality changes related to food quality observe the zero-order ($n = 0$) or first-order ($n = 1$) patterns [27]. The reaction formulas are as follows:

$$\begin{aligned} \text{zero} - \text{order reaction: } A &= A_0 - Kt, \\ \text{first} - \text{order reaction: } A &= A_0 \times e^{-Kt}, \end{aligned} \tag{2}$$

where A is the quality indicator, A_0 is the initial value of quality indicator, t is the storage time, and K is the reaction rate constant.

The average variation curve of the peel brittleness of stored melons is shown in Figure 6. The brittleness obviously decreased, which was consistent with the tendency of the zero-order reaction. Based on the peel brittleness prediction model and the spectral data of the first day collected by all samples, the initial values of the peel brittleness of samples in the first day could be predicted. In combination of the actually measured peel brittleness and storage time, the established zero-order reaction formula of stored melons was as follows:

$$A_t = 17.871 + 1.025A_0 - 24.814t, \tag{3}$$

where A_t is the storage peel brittleness value, A_0 is the initial value of peel brittleness, and t is the storage time. The

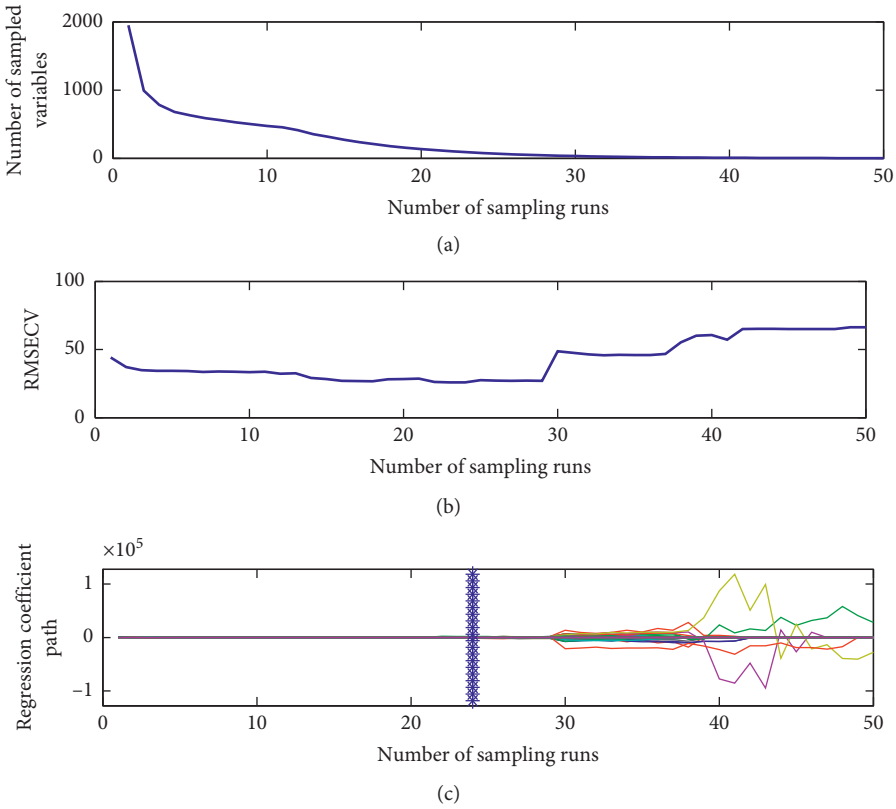

Figure 3: Feature wavelength selection via CARS.

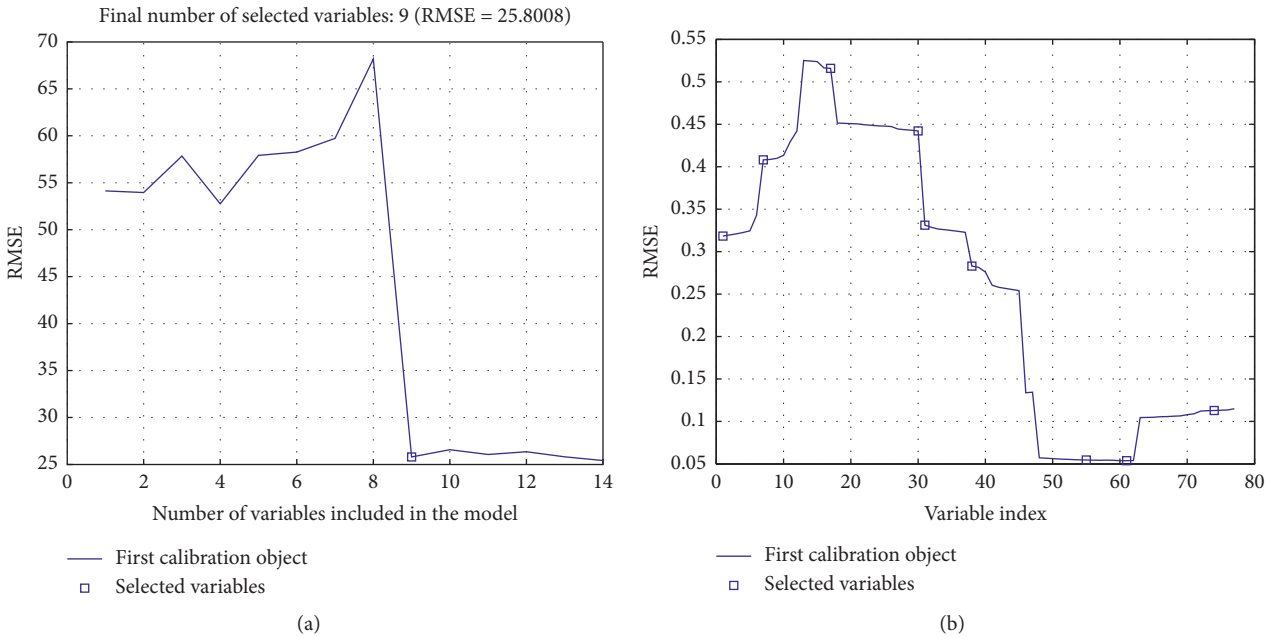

Figure 4: Feature wavelength selection via SPA.

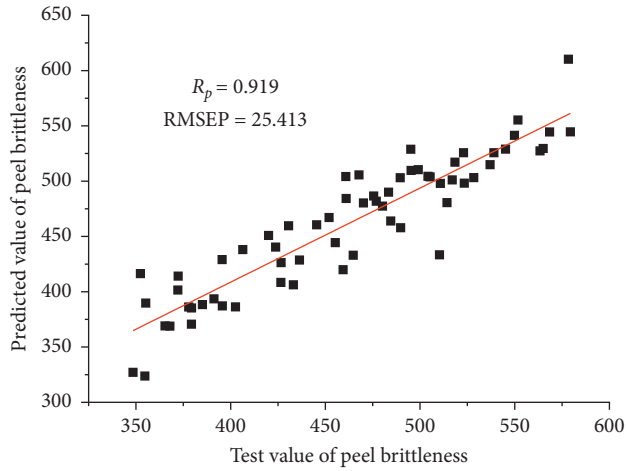

Figure 5: Prediction results of peel brittleness with the PLS model.

Table 3: Analysis of regression variance.

Sources of variance	DOF	Sum of squares	Mean square	F value	Pr > F Pr > F
Models	9	230643	25627	34.08	<0.0001
Errors	54	40609	752.01984	R^2 = 0.8503	
Total	63	271252			

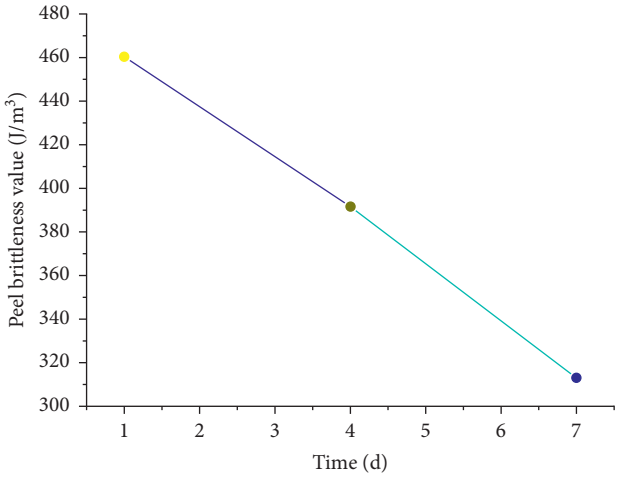

Figure 6: Change in curves of peel brittleness of Cucumis melons during storage.

model's correlation coefficient is 0.981, and the standard error is 4.624.

3.4. Establishment of Storage Time of Prediction Model. According to the zero-order reaction formula (3) of stored Cucumis melons, the expression equation of storage time is

$$t = 0.7202 + 0.0413A_0 - 0.0403A_t. \quad (4)$$

In combination of the expression of NIR peel brittleness of Cucumis melons (1), the relationship between the storage time t and the NIR absorbance level can be obtained, as shown below:

$$\begin{aligned} t = {} & 0.7202 + 0.0413\left(-4318.395X_1 + 4106.842X_2\right. \\ & -4215.299X_3 + 9399.809X_4 - 4438.19X_5 - 6481.062X_6 \\ & -20907X_7 + 11692X_8 + 11784X_9 + 527.963\left.\right) \\ & -0.0403\left(-4318.395X_{1t} + 4106.842X_{2t} - 4215.299X_{3t}\right. \\ & +9399.809X_{4t} - 4438.19X_{5t} - 6481.062X_{6t} \\ & -20907X_{7t} + 11692X_{8t} + 11784X_{9t} + 527.963\left.\right), \end{aligned} \quad (5)$$

where $X_{1t} - X_{9t}$ indicate the absorbance levels corresponding to all 9 feature wavelengths when the storage period is t.

4. Conclusions

Based on visible/near-infrared spectroscopy, the research established a kinetic model for peel brittleness of stored Cucumis melons and predicted the storage time. The research results are as follows:

(1) The NIR and peel brittleness values of melons stored for 1, 4, and 7 days are collected and measured, and pretreatment is conducted against the original spectrums. The results show that the reliability of the model pretreated with SG is the best. The correlation coefficients of calibration set and prediction set R_c^2 and R_p^2 are, respectively, 0.884 and 0.818, and RMSEC and RMSEP are, respectively, 22.205 and 23.775.

(2) CARS-SPA is adopted to extract feature wavelengths from the original spectrums, and 9 feature wavelengths are extracted at last, which are 1106, 841, 1340, 1917, 530, 1933, 1302, 2159, and 480 nm, in which the importance level descends in this order. Feature wavelengths are used to establish the peel brittleness PLS model, in which the prediction accuracy R_p is 0.919 and RMSEP is 25.413. With these 9 feature wavelengths, the NIR peel brittleness kinetic model of Cucumis melons is established and the determination coefficient is 0.8503, which realizes real-time inspection of the melons' peel brittleness.

(3) The zero-order reaction formula is created according to the variations in the peel brittleness of stored melons, the model's correlation coefficient is 0.981, and the standard error is 4.624. The linear relationship between the storage time of melons and NIR absorbance level can be obtained based on the NIR peel brittleness kinetic model and the zero-order reaction formula, thus achieving the nondestructive test of stored melons.

Data Availability

The data used to support the findings of this study are available from the corresponding author upon request.

Conflicts of Interest

The authors declare that they have no conflicts of interest.

Acknowledgments

This research was sponsored by the University Science and Technology Innovation Project of Shanxi, China (Project no. 2019L0402), Doctoral Research Project of Shanxi Agricultural University (Project no. 2018YJ43), and Excellent Doctor of Shanxi Province to Jin Work Award Fund Research Projects (Project no. SXYBKY2018030).

References

[1] R. Q. Yuan, L. Qian, W. J. Yun et al., "Cucurbitacins extracted from *Cucumis melo* L. (CuEC) exert a hypotensive effect via regulating vascular tone," *Hypertension Research*, vol. 42, no. 8, 2019.

[2] X. Chang, Z. Wang, and Z. Chen, "Optimization the storage technology of Jiashi muskmelon of Xinjiang by response surface methodology," *The Food Industry*, vol. 39, no. 4, pp. 70–73, 2018.

[3] L. D. C. Luiz, M. J. V. Bell, R. A. da Rocha, N. L. Leal, and V. de Carvalho dos Anjos, "Detection of veterinary antimicrobial residues in milk through near-infrared absorption spectroscopy," *Journal of Spectroscopy*, vol. 2018, Article ID 5152832, 6 pages, 2018.

[4] A. Peirs, A. Schenk, and B. M. Nicolaï, "Effect of natural variability among apples on the accuracy of VIS-NIR calibration models for optimal harvest date predictions," *Postharvest Biology and Technology*, vol. 35, no. 1, pp. 1–13, 2005.

[5] T. Ignat, S. Lurie, J. Nyasordzi et al., "Forecast of apple internal quality indices at harvest and during storage by VIS-NIR spectroscopy," *Food and Bioprocess Technology*, vol. 7, no. 10, pp. 2951–2961, 2014.

[6] J. Li, W. Huang, C. Zhao, and B. Zhang, "A comparative study for the quantitative determination of soluble solids content, pH and firmness of pears by vis/NIR spectroscopy," *Journal of Food Engineering*, vol. 116, no. 2, pp. 324–332, 2013.

[7] J. He, C. Qiao, D. Li et al., "Non-destructive detection of vitamin C content in "Lingwu Changzao" Jujubes (*Zizyphus jujuba* Mill.cv Lingwu Changzao) using visible near infrared hyperspectral imaging," *Food Science*, vol. 39, no. 6, pp. 194–199, 2018.

[8] S. Munera, C. Besada, N. Aleixos et al., "Non-destructive assessment of the internal quality of intact persimmon using colour and VIS/NIR hyperspectral imaging," *LWT*, vol. 77, pp. 241–248, 2017.

[9] H. Xiao, A. Li, M. Li et al., "Quality assessment and discrimination of intact white and red grapes from *Vitis vinifera* L. at five ripening stages by visible and near-infrared spectroscopy," *Scientia Horticulturae*, vol. 233, pp. 99–107, 2018.

[10] L. J. Janik, D. Cozzolino, R. Dambergs, W. Cynkar, and M. Gishen, "The prediction of total anthocyanin concentration in red-grape homogenates using visible-near-infrared spectroscopy and artificial neural networks," *Analytica Chimica Acta*, vol. 594, no. 1, pp. 107–118, 2007.

[11] Y. Liu, Y. Zhou, and Y. Pan, "Online quantitative analysis of soluble solids content in navel oranges using visible-near infrared spectroscopy and variable selection methods," *Journal of Innovative Optical Health Sciences*, vol. 7, no. 6, Article ID 1350065, 2014.

[12] M. Cirilli, A. Bellincontro, S. Urbani et al., "On-field monitoring of fruit ripening evolution and quality parameters in olive mutants using a portable NIR-AOTF device," *Food Chemistry*, vol. 199, no. 0308–8146, pp. 96–104, 2015.

[13] A. Saad, S. N. Jha, P. Jaiswal, N. Srivastava, and L. Helyes, "Non-destructive quality monitoring of stored tomatoes using VIS-NIR spectroscopy," *Engineering in Agriculture, Environment and Food*, vol. 9, no. 2, pp. 158–164, 2016.

[14] M. Valente, R. Leardi, G. Self, G. Luciano, and J. P. Pain, "Multivariate calibration of mango firmness using vis/NIR spectroscopy and acoustic impulse method," *Journal of Food Engineering*, vol. 94, no. 1, pp. 7–13, 2009.

[15] Z. Dongyan, X. Lu, W. Qingyan et al., "The optimal local model selection for robust and fast evaluation of soluble solid content in melon with thick peel and large size by vis-NIR spectroscopy," *Food Analytical Methods*, vol. 12, no. 1, pp. 136–147, 2018.

[16] J. A. Xia, Y. Yang, H. Cao, C. Han, D. Ge, and W. Zhang, "Visible-near infrared spectrum-based classification of apple chilling injury on cloud computing platform," *Computers and Electronics in Agriculture*, vol. 145, pp. 27–34, 2018.

[17] L. M. Kandpal, S. Lohumi, M. S. Kim, J.-S. Kang, and B.-K. Cho, "Near-infrared hyperspectral imaging system coupled with multivariate methods to predict viability and vigor in muskmelon seeds," *Sensors and Actuators B: Chemical*, vol. 229, pp. 534–544, 2016.

[18] X. Cao, H. Ren, X. Li et al., "Discrimination of winter Jujube's maturity using hyperspectral technique combined with characteristic wavelength and spectral indices," *Spectroscopy and Spectral Analysis*, vol. 38, no. 7, pp. 189–196, 2018.

[19] A. Polesello, R. Giangiacomo, and G. G. Dull, "Application of near infrared spectrophotometry to the nondestructive analysis of foods: a review of experimental results," *C R C Critical Reviews in Food Science and Nutrition*, vol. 18, no. 3, pp. 203–230, 1983.

[20] X. Zhao, S. Zhang, J. L. Liu et al., "Study on varieties discrimination of nectarine by hyperspectral technology combined with CARS-ELM algorithm," *Modern Food Science and Technology*, vol. 33, no. 10, pp. 281–287, 2017.

[21] M. Sun, D. Zhang, L. Liu, and Z. Wang, "How to predict the sugariness and hardness of melons: a near-infrared hyperspectral imaging method," *Food Chemistry*, vol. 218, pp. 413–421, 2017.

[22] H. Sun, S. Zhang, J. Xue et al., "Establishment and analysis of internal comprehensive quality spectral evaluation index for fresh Jujube," *Transactions of the Chinese Society for Agricultural Machinery*, vol. 48, no. 9, pp. 324–329, 2017.

[23] P. Maniwara, K. Nakano, D. Boonyakiat, S. Ohashi, M. Hiroi, and T. Tohyama, "The use of visible and near infrared spectroscopy for evaluating passion fruit postharvest quality," *Journal of Food Engineering*, vol. 143, no. 2, pp. 33–43, 2014.

[24] L. Pan, Q. Zhang, W. Zhang, Y. Sun, P. Hu, and K. Tu, "Detection of cold injury in peaches by hyperspectral reflectance imaging and artificial neural network," *Food Chemistry*, vol. 192, pp. 134–141, 2016.

[25] J. Shuying, J. Sun, Z. Xin, H. Mao, X. Wu, and Q. Li, "Visualizing distribution of pesticide residues in mulberry leaves using NIR hyperspectral imaging," *Journal of Food Process Engineering*, vol. 40, no. 4, 2016.

[26] S. Zhang, Z. Wang, X. Zou et al., "Recognition of tea disease spot based on hyperspectral image and genetic optimization neural network," *Transactions of the Chinese Society of Agricultural Engineering*, vol. 33, 2017.

[27] B. Ling, J. Tang, F. Kong, E. J. Mitcham, and S. Wang, "Kinetics of food quality changes during thermal processing: a review," *Food and Bioprocess Technology*, vol. 8, no. 2, pp. 343–358, 2015.